Progress In Electromagnetics Research, Vol. 136, 269–282, 2013

ENHANCED NONLINEARITIES IN DOUBLE-FISHNET NEGATIVE-INDEX PHOTONIC METAMATERIALS

Jun Guo[1], Yuanjiang Xiang[1, *], Xiaoyu Dai[2], and Shuangchun Wen[1]

[1]Key Laboratory for Micro-/Nano-Optoelectronic Devices of Ministry of Education, College of Physics and Microelectronic Science, Hunan University, Changsha 410082, China

[2] College of Electrical and Information Engineering, Hunan University, Changsha 410082, China

Abstract—We numerically analyze the optical response and nonlinear susceptibilities of fishnet metamaterials with the holes infiltrated by a third-order nonlinear dielectric. Through full-wave simulations and employing a nonlinear parameter retrieval method, we confirm and quantify the enhanced nonlinearities, showing bulk third-order nonlinear susceptibilities that are up to two orders of magnitude larger than the nonlinear dielectric. We also use the retrieved parameters to calculate the material figure of merits and the conversion efficiencies, showing material figure of merits up to two orders of magnitude larger and conversion efficiencies up to four orders of magnitude larger than the nonlinear dielectric alone. Though these results are calculated using one-unit-cell thick structures, the large magnitude of the enhancement still makes these structures attractive, allowing reasonable conversion efficiencies supported by even subwavelength slabs.

1. INTRODUCTION

Metamaterials (MMs) have attracted great attention due to their unusual electromagnetic properties not available in nature [1]. They have been exploited to develop unusual optical materials and devices, such as negative-index materials [2, 3] and "invisibility cloaks" [4, 5]. Negative-index MMs (NIMs) operating at optical frequencies have recently attracted considerable attention because of their novel

Received 6 December 2012, Accepted 11 January 2013, Scheduled 19 January 2013

* Corresponding author: Yuanjiang Xiang (xiangyuanjiang@126.com).

properties in optics [6–12]. One of the important NIM designs which is suitable for optical frequencies is the fishnet metal-dielectric-metal structure [13–18]. There have been considerable investigations on the linear optical properties of the fishnet structure during the past few years, such as the influence of the hole shape [19, 20], the effect of structure parameters [21] and tunability of the fishnet structures infiltrated with a nematic liquid crystal [22, 23].

Due to the strong local field enhancement within the MMs, there are new opportunities for enhanced nonlinear optical response. It was predicted that nonlinear MMs (NMMs) could provide a way not just to adopte the nonlinearities of their constituent materials but also to enhance them by orders of magnitude [24, 25]. A lot of research in NMMs have been done including demonstrations of frequency generation [26, 27], parametric amplification [28, 29], self-phase modulation and bistability [30, 31]. However, so far there are no works on nonlinear optical properties of realistic structures with negative index, such as the fishnet structures.

In this paper, we numerically analyze the nonlinear optical response of fishnet NMMs exhibiting negative refractive index. We study a structure with the holes infiltrated by a generic nonlinear dielectric and retrieve its nonlinearities using method described in [32–35]. We try to get varied nonlinear enhancement properties and identify the effects of varied structure parameters. These results are calculated using one-unit-cell thickness, which is limited by increasing linear absorption with increasing thickness, and assumption that the incident wavelength should be much larger than the thickness. However, the large magnitude of the enhancement still makes these structures attractive, allowing reasonable conversion efficiencies supported by even subwavelength slabs.

The paper is organized as follows. In Section 2, we introduce the method of analysis and present the simulated geometry. In Section 3, we discuss the simulation results in detail. Finally, in Section 4, we summarize our results and conclusions.

2. PROPOSED STRUCTURE AND SIMULATION METHOD

It is well known that fishnet structures are composed of two parts: an array of thin metal wires parallel to the direction of electric field, which can be treat as "electric atoms" and results the effective negative electric permittivity (ε), and a pair of finite-width metal stripes separated by a dielectric layer along the direction of the incident magnetic field, which can be treat as "magnetic atoms" and results the

effective negative magnetic permeability (μ). The resulting structure is a 2D array of holes penetrating completely through a metal-dielectric-metal film stack [13, 20], as is shown in Fig. 1(a).

Comparing to [14] and making the structure resonant near the near-infrared wavelength, we use structure parameters described in [14]. We keep the thickness of each layer constant, $t = 45\,\text{nm}$, $s = 30\,\text{nm}$, and the lattice constant, $a_x = a_y = 600\,\text{nm}$. If w_x =316 nm, $w_y = 100\,\text{nm}$, we will get the same structure described in Ref. [14] and the simulation results is completely the same. The retrieved linear properties are shown in Figs. 1(b) and (c). Fig. 1(b) shows the retrieved permittivity and permeability, and Fig. 1(c) is the retrieved refractive index. It is shown that the negative real part of permittivity and negative real part of permeability results a negative real part of refractive index. These results are exactly the same as those in [14].

The metal layers are silver, and the dielectric spacer is MgF_2. We use the free-electron Drude model with plasma frequency $\omega_{pl} = 1.37 \times 10^{16}\,\text{s}^{-1}$ and collision frequency $\omega_{col} = 8.5 \times 10^{13}\,\text{s}^{-1}$ for silver, which is the same as that in [14]. The refractive index of MgF_2 is $n = 1.38$. As is discussed in [14, 19], we know that the MM slab is

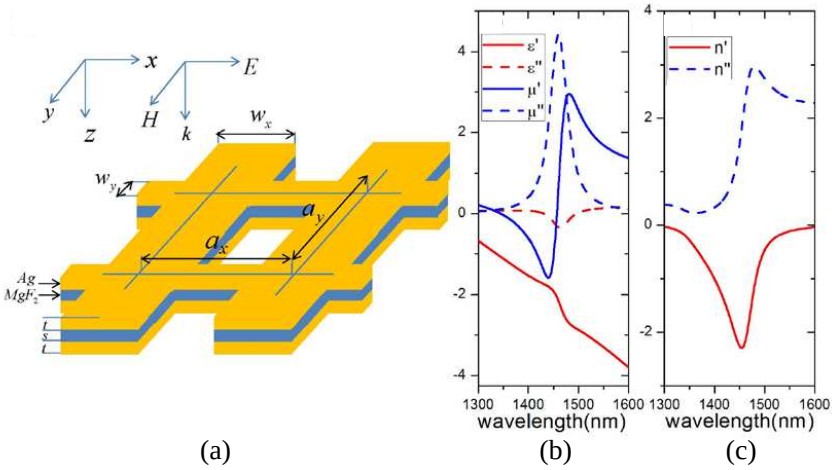

(a) (b) (c)

Figure 1. (a) Scheme of the negative-index metamaterial design and polarization configuration. The sample parameters are given: $w_x = 316\,\text{nm}$, $w_y = 100\,\text{nm}$, $t = 45\,\text{nm}$, $s = 30\,\text{nm}$, and lattice constant $a_x = a_y = 600\,\text{nm}$. (b) The real (solid) and imaginary (dashed) parts of retrieved permittivity (red) and magnetic permeability (blue). (c) The real (solid red) and imaginary (dashed blue) parts of retrieved refractive index.

usually located on a substrate in experiments, so the complex field reflectance for a wave incident from one side is generally not the same as that from the opposite side. To avoid this problem of asymmetric, we embed the structure in an effective homogeneous medium with refractive index 1.05.

Then we introduce the simulation method used in this work simply, our linear retrieval is based on [36, 37], and nonlinear retrieval is based on [33–35]. The validity of these simulations has been verified by repeating the results of these papers. For the full details of the existing nonlinear retrieval method, the reader is referred to [33–35]. We use FEM software to perform full-wave, frequency-domain simulations on a single unit cell of the fishnet structure. We use periodic boundary conditions to simulate a MM slab with infinite extend in the transverse direction. The nonlinear processes are considered by infiltrating the holes with a third-order nonlinear, or Kerr, dielectric. We calculate the fundamental and nonlinear scattered fields separately, the fundamental fields are solved first, neglecting the nonlinearity and then the fundamental fields is used to calculate the nonlinear polarization of the dielectric [35].

For all the simulations, the unit cell is excited by a plane wave traveling in the z direction, with the electric field polarized along the x axis. The linear properties are retrieved using the standard scattering-parameter retrieval techniques [36, 37], and the nonlinear scattered field are measured at the output and input ports and are used in the following retrieval process [33–35]. For the third-order nonlinearity, the retrieved parameters are the effective electric and magnetic third-order susceptibilities $\chi^{(3)}_{e,xxxx}$ and $\chi^{(3)}_{m,yyyy}$. Both electric and magnetic third-order susceptibilities can be retrieved despite that only electric third-order nonlinear dielectric was added in the fishnet structure, this is because the magnetic resonant nature of the MMs [35]. In the following, we assume the third-order susceptibilities of nonlinear dielectric in the holes to be $\chi^{(3)}_d$, and its refractive index n_d is 1.05. Note that the assumptions of n_d are mainly for illustrative purposes, and their magnitudes are unrealistic. For larger n_d, we need to increase w_y to make the fishnet metamaterial keep its negative refractive index and resonant at the desired wavelength.

At last, we are able to discuss the nonlinear response of the fishnet NLMMs. The same as discussing the effect of structure parameters on linear response in Ref. [21], we discuss two parameters' effect on the nonlinear response: (A) We fix w_y =100 nm and vary w_x. (B) We fix w_x =316 nm and vary w_y.

After we get the $\chi^{(3)}_{e,xxxx}$ and $\chi^{(3)}_{m,yyyy}$ for both the two cases, it is necessary to give a more thorough analysis to verify their applicability

in realistic nonlinear devices. It is necessary because in NLMMs the metallic inclusions generate most of the losses. The losses will constrain the maximum lengths of any resulting devices. So the enhancement effect must be compared with the losses. We introduce the figures of merit (FOM) for nonlinear devices defined in Ref. [35]. The effective material figure of merit is

$$\kappa^{(3)} = \frac{Z(\omega)^2}{Z_0}\chi_e^{(3)} + \frac{Z_0}{Z(\omega)^2}\chi_m^{(3)} \tag{1}$$

with units of m^2/W. Where $Z(\omega) = \sqrt{\mu(\omega)/\varepsilon(\omega)}$ is the effective impedance of the fishnet NLMMs and Z_0 is the impedance of free space. Then the corresponding material figure of merit of the nonlinear dielectric alone is

$$\kappa_d^{(3)} = \frac{Z_d^2}{Z_0}\chi_d^{(3)} \tag{2}$$

where the subscript d refers to the properties of the dielectric. Then follow the Ref. [35], we describe the third-order nonlinear process in terms of the intensity of the nonlinear scattered fields, given by

$$I_{\mathrm{out}}^{NL}(\omega) = \frac{9}{16}\frac{\omega^2}{c^2}\left|\kappa^{(3)}\right|^2 L^2 g\left(L\right)\left[I_{\mathrm{in}}^{FF}(\omega)\right]^3 \tag{3}$$

where

$$g\left(L\right) = \exp\left[-2\alpha(\omega)L\right] \tag{4}$$

contains the effect of propagation losses on efficiency. $\alpha(\omega)$ is the linear absorption of the fishnet NMMs, and $\alpha = 2\pi \times \mathrm{Im}(n_{eff}) \times \omega/c$ where $n_{eff} = \sqrt{\varepsilon_{eff}}$ is the effective linear refractive index and $\mathrm{Im}(\cdot)$ means imaginary parts. Then the conversion efficiency is given by the ratio of nonlinear scattered intensity to the input intensity

$$\eta^{(3)} = \frac{I_{\mathrm{out}}^{NL}(\omega)}{I_{\mathrm{in}}^{FF}(\omega)} = \frac{9}{16}\frac{\omega^2}{c^2}\left|\kappa^{(3)}\right|^2 L^2 g\left(L\right)\left[I_{\mathrm{in}}^{FF}(\omega)\right]^2 \tag{5}$$

And it can be normalized by the efficiency of the dielectric alone, and get the figure of merit describing the enhancement of third-order nonlinear process:

$$F\left(\eta^{(3)}\right) = \frac{\eta^{(3)}}{\eta_d^{(3)}} = g\left(L\right)\left|\frac{\kappa^{(3)}}{\kappa_d^{(3)}}\right|^2 \tag{6}$$

Note that in Ref. [35], they calculate the conversion efficiency using $L_{\mathrm{opt}} = \frac{1}{\alpha(\omega)}$, which is the optimum interaction length found by maximizing the quantity $L^2 g(L)$. In our work, however, we have the

fishnet structure whose thickness is fixed, so we calculate the conversion efficiency using fixed interaction length $L = 120\,\text{nm}$.

After these settings, we are able to discuss the third-order nonlinear process of the fishnet structures systematically and also give a more thorough analysis of them in terms of their applicability in realistic nonlinear devices.

3. RESULTS AND DISCUSSION

First to describe the linear optical properties of the fishnet NMMs, we choose linear absorption as a representative. Linear properties such as negative refractive index and transmission have been largely discussed in Refs. [19–21], and it is not our purpose here. We will not study these properties, however the parameters we choose here always make the fishnet NMMs have a negative refractive index in the chosen spectrum. We choose linear absorption as a representative because the introduction of metallic inclusions in MMs will surely increase its linear absorption which impedes its potential applications, so it is necessary to discuss its linear absorption quantitatively. Meanwhile the linear absorption can also reveal the MMs linear optical properties, such as the resonant wavelength and absorption peak. Fig. 2 shows the linear absorption curves for both the two cases discussed in Section 2. Figs. 2(a) and (b) are for case (A) and (B) respectively. In case (A),

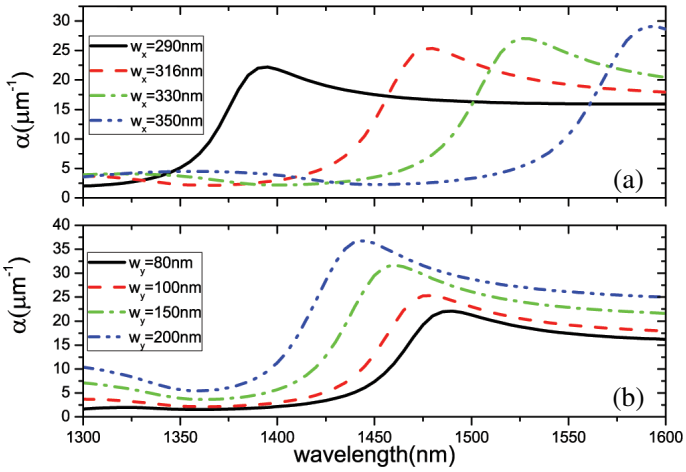

Figure 2. (a) Wavelength dependent linear absorption curves for different w_x in case (A). (b) Wavelength dependent linear absorption curves for different w_y in case (B).

we fix the $w_y = 100\,\text{nm}$ and vary w_x to be 290 nm, 316 nm, 330 nm and 350 nm, the linear absorption is shown in Fig. 2(a). The resonant wavelength red-shifts with the increase of width of "magnetic atoms", w_x, and the maximum absorption increases slightly. This red-shift of resonant wavelength can be qualitatively explained by tracking the resonance of an equivalent L-C circuit: a wider grating corresponds to larger inductance and capacitance, which in turn leads to a larger resonance wavelength [21]. And due to the increased fill fraction of metallic inclusions, the absorption will increase simultaneously. In case (B), we fix the w_x =316 nm and vary w_y to be 80 nm, 100 nm, 150 nm and 200 nm, the linear absorption is shown in Fig. 2(b). With the increase of width of "electric atoms", w_y, the resonant wavelength blue-shifts indicating an interaction between the electric and magnetic structures and the maximum absorption also increases. As is well known, the "electric atoms" mainly provide an effective negative electric permittivity, with the increase of width of "electric atoms", magnitude of the effective negative electric permittivity becomes larger and induce increased imaginary refractive index (not shown here). Thus the linear absorption will increase.

Then we consider the fishnet NMMs' nonlinear enhancement properties for both the two cases, as is discussed in Section 2. For case (A), in Fig. 3 we show the retrieved nonlinearities of both electric and magnetic contributions, allowing for the complete characterization of the fishnet NMMs. Figs. 3(a) and (b) show the real and imaginary part of the electric susceptibilities, normalized by the nonlinear bulk dielectric. Figs. 3(c) and (d) show the real and imaginary part of the magnetic susceptibilities, normalized by the nonlinear bulk dielectric. The magnetic susceptibilities are also normalized by the impedance of free space where appropriate [35]. As expected, the retrieved nonlinearities of the fishnet NMMs are highly enhanced near the resonance. The retrieved nonlinear susceptibilities also show the Lorentzian features in their real and imaginary parts. Note that the magnetic properties have roughly a π phase relation with the corresponding electric properties, akin to the "antiresonance" features common to linear MMs retrievals [35]. As the w_x increases, the maximum magnitude of electric susceptibilities increases while the maximum magnitude of magnetic susceptibilities decreases indicating increased electric response and decreased magnetic response in the fishnet NMMs. And the resonant wavelength shows red-shifts which is the same as the linear absorption. The magnitude of the normalized magnetic susceptibilities is several times larger than the normalized electric susceptibilities indicating that with these parameters the fishnet NMMs are mostly magnetic in nature.

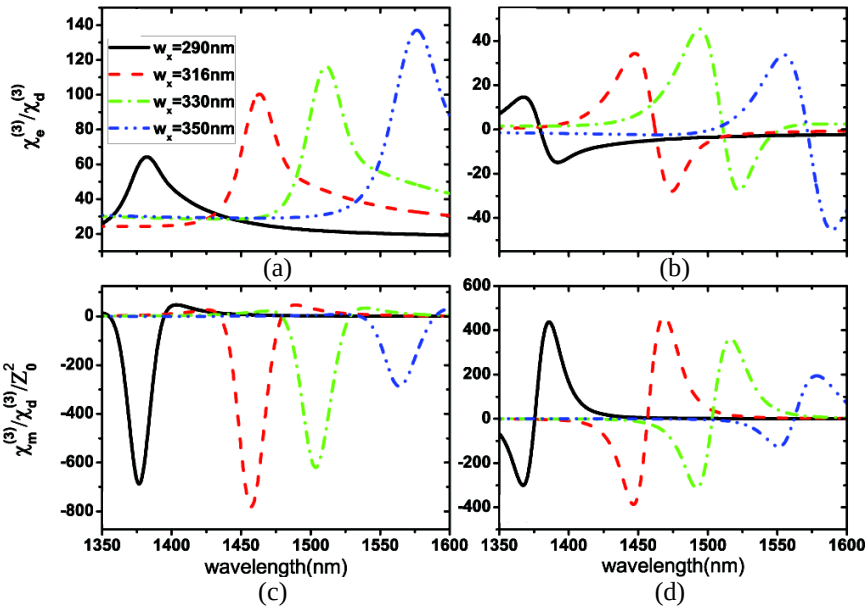

Figure 3. (a) Real and (b) imaginary parts of the electric susceptibilities for case (A), normalized by the nonlinear bulk dielectric. (c) Real and (d) imaginary parts of the magnetic susceptibilities for case (A), normalized by the nonlinear bulk dielectric and the impedance of free space.

For case (B), in Fig. 4 we show the retrieved nonlinearities of both electric and magnetic contributions. Figs. 4(a) and (b) show the real and imaginary part of the electric susceptibilities, Figs. 4(c) and (d) show the real and imaginary part of the magnetic susceptibilities, both are normalized by the nonlinear bulk dielectric. The retrieved nonlinear susceptibilities are similar to those in case (A). However, as w_y increases, the maximum magnitude of electric susceptibilities increases and the maximum magnitude of magnetic susceptibilities decrease significantly. When $w_y = 80\,\text{nm}$ and $100\,\text{nm}$, the magnitude of the normalized magnetic susceptibilities is several times larger than the normalized electric susceptibilities indicating that with these parameters the fishnet NMMs are mostly magnetic in nature. However, this is different when w_y is larger, such as $w_y = 200\,\text{nm}$, the magnitude of the normalized electric susceptibilities is much larger than the normalized magnetic susceptibilities indicating that the fishnet NMMs are mostly electric in nature. The resonant wavelength shows blue-shifts which is the same as the linear absorption.

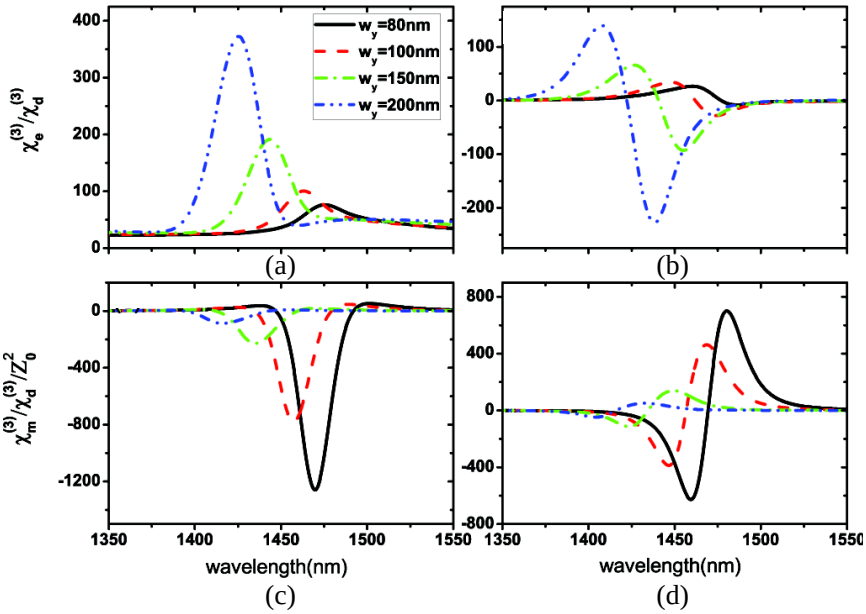

Figure 4. (a) Real and (b) imaginary parts of the electric susceptibilities for case (B), normalized by the nonlinear bulk dielectric. (c) Real and (d) imaginary parts of the magnetic susceptibilities for case (B), normalized by the nonlinear bulk dielectric and the impedance of free space.

The retrieved parameters of the previous discussion fully characterize the fishnet NMMs, thus we are in position to analysis their applicability in realistic nonlinear devices. We will use FOM introduced in Section 2 to give a more thorough analysis of the fishnet NLMMs. First in Fig. 5, we show the material FOM $|\kappa^{(3)}/\kappa_d^{(3)}|$, which do not include the linear absorption, also normalized by the nonlinear bulk dielectric. Fig. 5(a) shows curves for case (A) and Fig. 5(b) is for case (B). For both the two cases, the material FOM show peak values that are two orders of magnitude larger than the embedding nonlinear dielectric alone. For case (A), as w_x increases, the peak value of material FOM increases first and then decreases, showing maximum magnitude near w_x =316 nm. While for case (B), as w_y increases, the peak value of material FOM decreases even if there are no linear absorption involved. So we can expect that considering increased linear absorption for case (B), the conversion efficiencies will decrease more rapidly as w_y increases. While the material FOM is the lowest when $w_y = 200$ nm, it has the largest electric susceptibilities.

Then we take linear absorption into account, as is discussed in Section 2. In Fig. 6 we show the conversion efficiencies of the third-order nonlinearities where linear absorption is involved, normalized by the efficiency of the dielectric alone. For both the two cases, the conversion efficiencies show peak values that are four orders of magnitude larger than the embedding nonlinear dielectric alone. For case (A), as w_x increases, the peak value of conversion efficiencies increases first and then decreases, showing maximum magnitude near $w_x = 316\,\text{nm}$. While for case (B), as w_y increases, the peak value of conversion efficiencies decreases rapidly due to the increased linear absorption. The resonant nature of the fishnet structures results a narrow band of operation as well as relatively large losses. Thus, applications will likely be constrained to slabs only a few unit cells thick, in our work it is only a unit cell thick and $L = 120\,\text{nm}$. If we make the thickness L larger, there will be rapid reduction of conversion efficiencies. However, the magnitude of the enhancement still makes these structures attractive, allowing even subwavelength slabs to support reasonable conversion efficiencies. And additionally, the fishnet structure have refractive index which can be positive, near-zero or even negative, so there emerge new opportunities for intriguing properties.

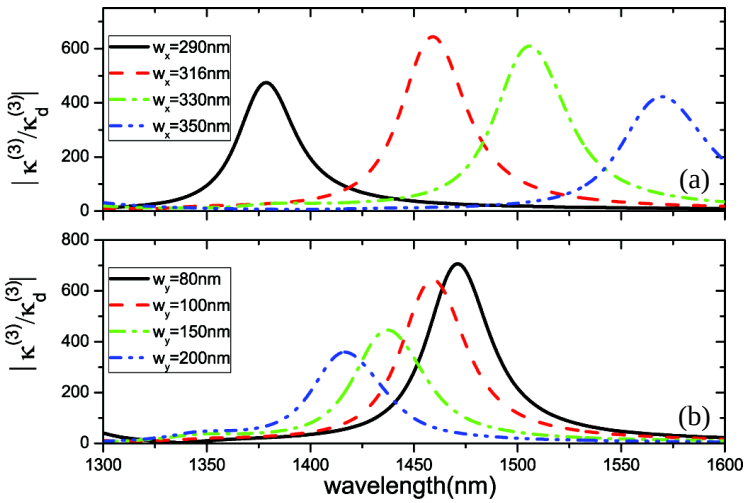

Figure 5. (a) Normalized material FOM $\left|\kappa^{(3)}/\kappa_d^{(3)}\right|$ for case (A). (b) Normalized material FOM $\left|\kappa^{(3)}/\kappa_d^{(3)}\right|$ for case (B).

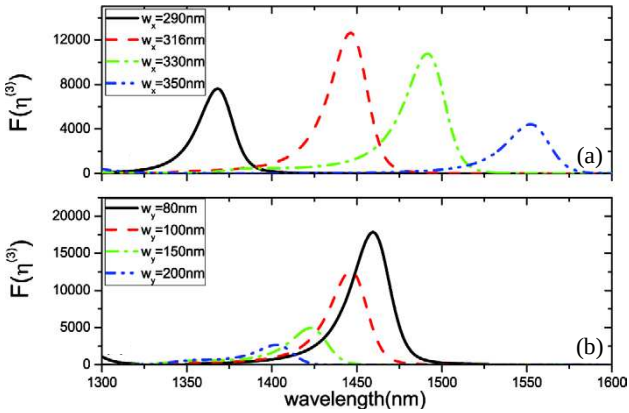

Figure 6. (a) Normalized conversion efficiencies $F\left(\eta^{(3)}\right)$ for case (A). (b) Normalized conversion efficiencies $F\left(\eta^{(3)}\right)$ for case (B).

4. CONCLUSION

In conclusion, we have demonstrated in this work, through full-wave simulations and by employing the nonlinear retrieval method, a quantitative analysis of the enhancement of the effective nonlinearities of fishnet MMs with the holes infiltrated by a third-order nonlinear dielectric. The fishnet NMMs can support both enhanced electric and magnetic nonlinearities compared to the electric nonlinear dielectric, with improvements as high as two orders of magnitude for the third-order material figures of merit. Such enhancements, together with the unique and configurable properties of fishnet MMs, have the potential applications in a new generation of efficient and compact nonlinear devices.

ACKNOWLEDGMENT

This work is supported by the National Natural Science Foundation of China (Grant No. 11004053), the China Postdoctoral Science Foundation (Grant No. 2012M511365), the Ph.D. Programs Foundation of Ministry of Education of China (Grant No. 20120161120013), and the Young Teacher Development Plan of Hunan University.

REFERENCES

1. Pendry, J. B., D. Schurig, and D. R. Smith, "Controlling electromagnetic fields," *Science*, Vol. 312, No. 1780, 1780–1782, 2006.

2. Smith, D. R., W. J. Padilla, D. C. Vier, S. C. Nemat-Nasser, and S. Schultz, "Composite medium with simultaneously negative permeability and permittivity," *Phys. Rev. Lett.*, Vol. 84, No. 18, 4184–4187, 2000.
3. Shelby, R. A., D. R. Smith, and S. Schultz, "Experimental verification of a negative index of refraction," *Science*, Vol. 292, No. 5514, 77–79, 2001.
4. Schurig, D., J. J. Mock, B. J. Justice, S. A. Cummer, J. B. Pendry, A. F. Starr, and D. R. Smith, "Metamaterial electromagnetic cloak at microwave frequencies," *Science*, Vol. 314, No. 5801, 977–980, 2006.
5. Shao, J., H. Zhang, Y. Lin, and H. Xin, "Dual-frequency electromagnetic cloaks enabled by LC-based metamaterial circuits," *Progress In Electromagnetics Research*, Vol. 119, 225–237, 2011.
6. Shalaev, V. M., "Optical negative-index metamaterials," *Nature Photon.*, Vol. 1, 41–48, 2006.
7. Soukoulis, C. M., S. Linden, and M. Wegener, "Negative refractive index at optical wavelengths," *Science*, Vol. 315, 47–49, 2007.
8. Busch, K., G. von Freymann, S. Linden, S. Mingaleev, L. Tkeshelashvili, and M. Wegener, "Periodic nanostructures for photonics," *Phys. Rep.*, Vol. 444, No. 3, 101–202, 2007.
9. Oraizi, H., A. Abdolali, and N. Vaseghi, "Application of double zero metamaterials as radar absorbing materials for the reduction of radar cross section," *Progress In Electromagnetics Research*, Vol. 101, 323–337, 2010.
10. Duan, Z., Y. Wang, X. Mao, W.-X. Wang, and M. Chen, "Experimental demonstration of double-negative metamaterials partially filled in a circular waveguide," *Progress In Electromagnetics Research*, Vol. 121, 215–224, 2011.
11. Li, J., F.-Q. Yang, and J. Dong, "Design and simulation of L-shaped chiral negative refractive index structure," *Progress In Electromagnetics Research*, Vol. 116, 395–408, 2011.
12. Canto, J. R., C. R. Paiva, and A. M. Barbosa, "Dispersion and losses in surface waveguides containing double negative or chiral metamaterials," *Progress In Electromagnetics Research*, Vol. 116, 409–423, 2011.
13. Zhang, S., W. Fan, N. C. Panoiu, K. J. Malloy, R. M. Osgood, and S. R. J. Brueck, "Experimental demonstration of near-infrared negative-index metamaterials," *Phys. Rev. Lett.*, Vol. 95, 137404, 2005.

14. Dolling, G., C. Enkrich, M. Wegener, C. M. Soukoulis, and S. Linden, "Low-loss negative-index metamaterial at telecommunication wavelengths," *Opt. Lett.*, Vol. 31, No. 12, 1800–1802, 2006.
15. Chettiar, U. K., A. V. Kildishev, H.-K. Yuan, W. Cai, S. Xiao, V. P. Drachev, and V. M. Shalaev, "Dual-band negative index metamaterial: Double negative at 813 nm and single negative at 772 nm," *Opt. Lett.*, Vol. 32, No. 12, 1671–1673, 2007.
16. Li, T., J.-Q. Li, F.-M. Wang, Q.-J. Wang, H. Liu, S.-N. Zhu, and Y.-Y. Zhu, "Exploring magnetic plasmon polaritons in optical transmission through hole arrays perforated in trilayer structures," *Appl. Phys. Lett.*, Vol. 90, No. 25, 251112, 2007.
17. Valentine, J., S. Zhang, T. Zentgraf, E. Ulin-Avila, D. A. Genov,G. Bartal, and X. Zhang, "Three-dimensional optical metamaterial with a negative refractive index," *Nature*, Vol. 455, 376–379, 2008.
18. Minovich, A., D. N. Neshev, D. A. Powell, I. V. Shadrivov, M. Lapine, H. T. Hattori, H. H. Tan, C. Jagadish, and Yu. S. Kivshar, "Tilted response of fishnet metamaterials at near-infrared optical wavelengths," *Phys. Rev. B*, Vol. 81, No. 11, 115109, 2010.
19. Dolling, G., M. Wegener, C. M. Soukoulis, and S. Linden, "Design-related losses of double-fishnet negative-index photonic metamaterials," *Opt. Express*, Vol. 15, No. 18, 11536–11538, 2007.
20. Ku, Z. and S. R. J. Brueck, "Comparison of negative refractive index materials with circular, elliptical and rectangular holes," *Opt. Express*, Vol. 15, No. 8, 4515–4522, 2007.
21. Zhang, S., W. Fan, K. J. Malloy, S. R. J. Brueck, N. C. Panoiu, and R. M. Osgood, "Near-infrared double negative metamaterials," *Opt. Express*, Vol. 13, No. 13, 4922–4930, 2005.
22. Minovich, A., D. N. Neshev, D. A. Powell, and I. V. Shadrivov, "Tunable fishnet metamaterials infiltrated by liquid crystals," *Appl. Phys. Lett.*, Vol. 96, No. 19, 193103, 2010.
23. Wang, X., D.-H. Kwon, D. H. Werner, I.-C. Khoo, A. V. Kildishev, and V. M. Shalaev, "Tunable optical negative-index metamaterials employing anisotropic liquid crystals," *Appl. Phys. Lett.*, Vol. 91, No. 14, 143122, 2007.
24. Pendry, J. B., A. J. Holden, D. J. Robbins, and W. J. Stewart, "Magnetism from conductors and enhanced nonlinear phenomena," *IEEE Trans. Microwave Theory*, Vol. 47, No. 11, 2075–2084, 1999.

25. Zharov, A. A., I. V. Shadrivov, and Y. S. Kivshar, "Nonlinear properties of left-handed metamaterials," *Phys. Rev. Lett.*, Vol. 91, No. 3, 037401, 2003.
26. Klein, M. W., C. Enkrich, M. Wegener, and S. Linden, "Second-harmonic generation from magnetic metamaterials," *Science*, Vol. 313, No. 5786, 502–504, 2006.
27. Shadrivov, I. V., A. B. Kozyrev, D. W. van der Weide, and Y. S. Kivshar, "Tunable transmission and harmonic generation in nonlinear metamaterials," *Appl. Phys. Lett.*, Vol. 93, No. 16, 161903, 2008.
28. Popov, A. and V. Shalaev, "Negative-index metamaterials: Second-harmonic generation, Manley-Rowe relations and parametric amplification," *Appl. Phys. B*, Vol. 84, No. 1, 131–137, 2006.
29. Poutrina, E., S. Larouche, and D. R. Smith, "Parametric oscillator based on a single-layer resonant metamaterial," *Opt. Commun.*, Vol. 283, No. 8, 1640–1646, 2010.
30. Powell, D. A., I. V. Shadrivov, Y. S. Kivshar, and M. V. Gorkunov, "Self-tuning mechanisms of nonlinear split-ring resonators," *Appl. Phys. Lett.*, Vol. 91, No. 14, 144107, 2007.
31. Shadrivov, I. V., A. B. Kozyrev, D. W. van der Weide, and Y. S. Kivshar, "Nonlinear magnetic metamaterials," *Opt. Express*, Vol. 16, No. 25, 20266–20271, 2008.
32. Rose, A., D. Huang, and D. R. Smith, "Controlling the second harmonic in a phase-matched negative-index metamaterial," *Phys. Rev. Lett.*, Vol. 107, No. 6, 063902, 2011.
33. Larouche, S. and D. R. Smith, "A retrieval method for nonlinear metamaterials," *Opt. Commun.*, Vol. 283, No. 8, 1621–1627, 2010.
34. Rose, A., S. Larouche, D. Huang, E. Poutrina, and D. R. Smith, "Nonlinear parameter retrieval from three-and four-wave mixing in metamaterials," *Phys. Rev. E*, Vol. 82, No. 3, 036608, 2010.
35. Rose, A., S. Larouche, and D. R. Smith, "Quantitative study of the enhancement of bulk nonlinearities in metamaterials," *Phys. Rev. A*, Vol. 84, No. 5, 053805, 2011.
36. Smith, D. R., S. Schultz, P. Markos, and C. M. Soukoulis, "Determination of effective permittivity and permeability of metamaterials from reflection and transmission coefficients," *Phys. Rev. B*, Vol. 65, No. 19, 195104, 2002.
37. Smith, D. R., D. C. Vier, T. Koschny, and C. M. Soukoulis, "Electromagnetic parameter retrieval from inhomogeneous metamaterials," *Phys. Rev. E*, Vol. 71, No. 3, 036617, 2005.